


Crystallographic Snapshots of Tom20—Mitochondrial Presequence Interactions with Disulfide-Stabilized Peptides

Takashi Saitoh,[†] Mayumi Igura,[†] Yusuke Miyazaki,[†] Toyoyuki Ose,^{†,||} Nobuo Maita,[‡] and Daisuke Kohda^{*,†,§}

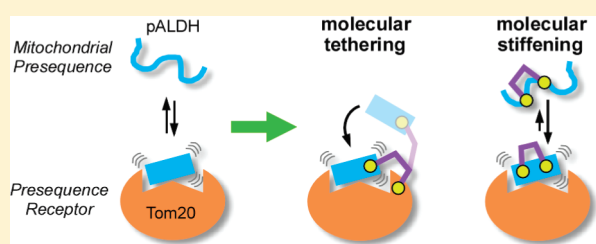
[†]Division of Structural Biology, Medical Institute of Bioregulation, Kyushu University, Maidashi 3-1-1, Higashi-ku, Fukuoka 812-8582, Japan

[‡]Institute for Enzyme Research, Tokushima University, 2-24, Shinkura-cho, Tokushima 770-8501, Japan

[§]Research Center for Advanced Immunology, Kyushu University, Maidashi 3-1-1, Higashi-ku, Fukuoka 812-8582, Japan

 Supporting Information

ABSTRACT: Most mitochondrial proteins are synthesized in the cytosol and imported into mitochondria. The Tom20 protein, residing on the mitochondrial surface, recognizes the N-terminal presequences of precursor proteins. We previously determined the crystal structures of the Tom20—presequence complex. The successful crystallization involved tethering the presequence to Tom20 through an intermolecular disulfide bond with an optimized linker. In this work, we assessed the tethering method. The intermolecular disulfide bond was cleaved *in crystal* with a reducing agent. The pose (i.e., conformation and position) of the presequence was identical to the previously determined pose. In another experiment, a longer linker than the optimized length was used for the tethering. The perturbation of the tether changed the pose slightly, but the interaction mode was preserved. These results argue against the forced interaction of the presequence by its covalent attachment to Tom20. Second, as an alternative method referred to as “molecular stiffening”, we introduced a disulfide bond within the presequence peptide to restrict the freedom of the peptide in the unbound states. One presequence analogue exhibited over 100-fold higher affinity than its linear counterpart and generated cocrystals with Tom20. One of the two crystallographic snapshots revealed a known pose previously determined by the tethering method, and the other snapshot depicted a new pose. These results confirmed and extended the dynamic, multiple bound state model of the Tom20—presequence interactions and also demonstrated the validity of the molecular tethering and stiffening techniques in studies of transient protein—peptide interactions.



Strict specificities in protein—protein interactions are essential in many biological processes. Such highly specific interactions are frequently monogamous with a special target and occur on the basis of shape and charge complementarity at the molecular interface. In contrast, polygamous binding (i.e., promiscuous or multispecific binding) to a set of diverse targets is also critically important in biological processes, such as intracellular protein sorting systems.^{1–5} Such promiscuous interactions require a special molecular mechanism to achieve comparable affinity for different targets, irrespective of their divergent properties. Recent reviews focused on the specificity versus promiscuity of protein—protein interactions highlighted the molecular mechanisms that fulfill such complicated requirements.^{6,7} One mechanism relies on large residual fluctuations in the bound state. Conventional analytical techniques, such as X-ray crystallography and NMR, have limitations in generating an atomic level perspective of structural information from bound states with large residual mobility. Frequently, the interaction of a promiscuous protein and its targets is weak in the micromolar to millimolar range, but the weak affinity does not directly hamper structural analyses at atomic resolutions. In fact, information on the bound state was obtained even from an extremely weak interaction ($K_d \sim 3$ mM) between an SH3 domain and a LIM domain by intermolecular NOEs using NMR spectroscopy.⁸

Even if substantial residual motion exists in the bound states, an equilibrium shift from the free state to the bound state can be achieved by introducing an intermolecular covalent bond between a protein and its ligand. Ideally, the perturbation of the residual mobility in the bound states should be minimized. If the ligand is a protein or peptide, then it can be fused to either the N- or C-terminus of the protein or tethered by an intermolecular disulfide bond between the protein and the partner protein/peptide. An obvious difficulty is the appropriate design of either the fusion proteins (N- or C-terminal fusion with a spacer of an appropriate length) or the disulfide-tethered complexes (the positions of the two cysteine residues in the primary structures) without any detailed structural information. Nonetheless, there are several successful examples that led to high-resolution crystal structures of the complexes.^{9–18}

Tom20, a 20 kDa subunit of the TOM (translocase of outer mitochondrial membrane) complex, is anchored to the mitochondrial outer membrane by its N-terminal hydrophobic

Received: March 29, 2011

Revised: May 13, 2011

Published: May 17, 2011

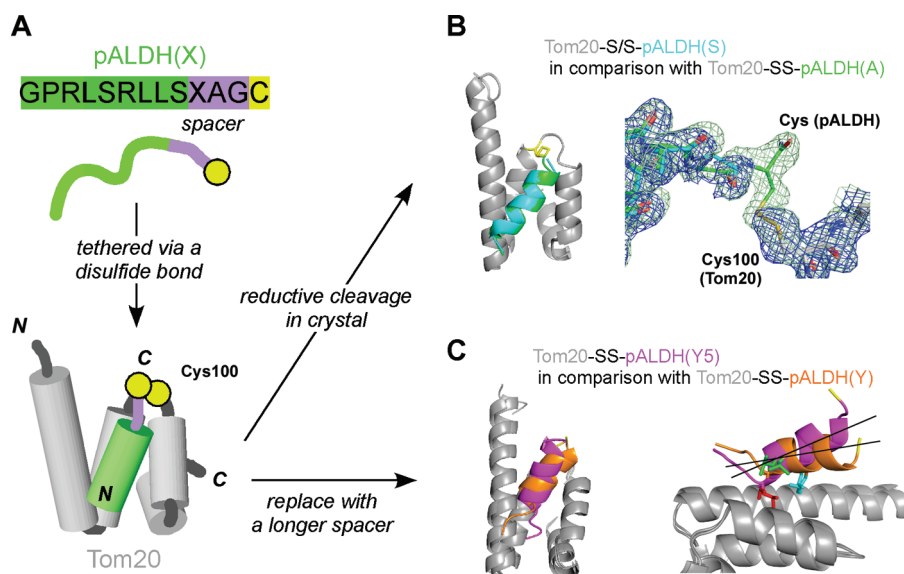


Figure 1. Crystal structures of disulfide bond tethered complexes of Tom20 and the presequence (pALDH) of aldehyde dehydrogenase, specially designed to verify the effects of tethering. (A) Schematic diagram of the disulfide bond tethering of a presequence peptide to Tom20. The amino acid sequence from pALDH is shown in green. A cysteine residue (yellow) was attached to the C-terminus after the three-residue spacer (purple). The amino acid at the X-position is explicitly shown in parentheses. The core structure of the cytosolic domain of Tom20 consists of four α -helices (gray). The intermolecular disulfide bond was formed with the single cysteine residue (Cys100, yellow circle) of Tom20. (B) Superposition of the structures of Tom20-S/S-pALDH(S) and Tom20-SS-pALDH(A). The 73 C α atoms of Tom20 were superimposed, with a root-mean-square (rms) distance of 0.22 Å. The intermolecular disulfide bond was cleaved by reduction in the crystal of Tom20-SS-pALDH(S), before the diffraction measurement. The $2F_o - F_c$ electron density maps at a contour level of 1.0 σ show that the electron density of the C-terminal cysteine residue in the Tom20-S/S-pALDH(S) structure disappeared, but those of the other residues in the presequence peptide were left undisturbed. (C) Superposition of the structures of Tom20-SS-pALDH(Y5) and Tom20-SS-pALDH(Y). The 70 C α atoms of Tom20 were superposed with an rms distance of 1.4 Å. Although the pose of the presequence was different, the three side chains (red, green, cyan) of the leucine residues of the presequence occupy similar positions in the two structures.

segment, and its C-terminal globular domain is exposed to the cytosol, in animals and fungi.^{19,20} The cytosolic domain of Tom20 interacts with the N-terminal portions of most, and likely all, mitochondrial precursor proteins destined for the mitochondrial matrix and inner membrane and thereby functions as a general receptor for preproteins.⁵ These N-terminal cleavable segments are collectively referred to as mitochondrial presequences. A presequence typically consists of 15–50 amino acid residues, with an abundance of positively charged residues, and tends to form an amphiphilic helical conformation.²¹ Contrary to expectations, the mitochondrial presequences lack obvious common sequence motifs. Thus, Tom20 binding to mitochondrial presequences is an example of a promiscuous interaction. The molecular mechanism by which the Tom20 protein distinguishes about 1000 (yeast) to 1500 (human) mitochondrial proteins from nonmitochondrial proteins and sorts them into mitochondria^{19,20} is an important biological subject.

Our previous NMR titration and peptide library experiments revealed that the consensus motif for the yeast and rat Tom20s comprised a five-residue consensus motif, $\phi\chi\chi\phi\phi$ (where ϕ is a hydrophobic amino acid and χ is any amino acid).^{22,23} A long presequence may contain two Tom20-binding motifs to increase the import efficiency.²⁴ We determined the NMR structure of the cytosolic domain (residues 51–145) of rat Tom20 in a complex with a presequence peptide, derived from the precursor of rat mitochondrial aldehyde dehydrogenase (ALDH).²⁵ The cytosolic domain of Tom20 consists of four α -helices with a loosely attached fifth α -helix and contains one typical tetratricopeptide repeat (TPR) motif. The bound portion (residues 15–19,

LSRLL) of the presequence peptide adopts an amphiphilic helical structure and is accommodated in the hydrophobic binding groove of Tom20. We tethered the presequence peptide onto Tom20 via an intermolecular disulfide bond²² by adding a cysteine residue at the C-terminus of the presequence peptide for this purpose (Figure 1A). The length of the spacer between the presequence and the C-terminal cysteine was optimized by a peptide library experiment using intermolecular disulfide bond formation.²² On the other hand, the cysteine residue in the original sequence of Tom20 was used for tethering. Two crystalline forms of the complex were obtained, with different spacer sequence designs.²⁶ The crystal structures are regarded as snapshots of the dynamic protein structure in solution. Here, a “pose” is defined as one ligand conformation and its position relative to the protein; that is, in the case of Tom20–presequence interactions, the orientation of the α -helical axis of the presequence relative to Tom20. The two crystal structures provided unique poses, and neither pose could fully account for the simultaneous requirement of the three hydrophobic side chains at the three ϕ positions in the consensus motif.²⁷ A dynamic equilibrium probably exists among the two and possibly more poses in solution. We propose that the dynamic, multiple-mode interaction is the molecular mechanism that facilitates the promiscuous binding of the Tom20 receptor to diverse mitochondrial presequences with similar affinities.

In plants, the counterpart of the animal and fungal Tom20s is C-terminally anchored to the mitochondrial outer membrane.²⁸ NMR analyses revealed that the cytosolic domain of the plant *Arabidopsis* Tom20 is a helical bundle consisting of

seven α -helices.²⁹ NMR titration experiments using stable isotope-labeled *Arabidopsis* Tom20 suggested that a groove in the concave surface, formed by two variants of the TPR motif, accommodated presequence peptides from *Arabidopsis* and yeast. Considering the sequence and structure analyses, the plant Tom20 is functionally equivalent to the animal and fungal Tom20s but arose independently after the divergence of animals and fungi from plants.²⁸ Subsequent NMR titration experiments using the labeled presequence peptides suggested that the plant Tom20 recognized short motifs, AIFVAK and LRALYG, which possessed a similar pattern (underlined) to the rat and yeast Tom20-binding motifs.³⁰ Molecular dynamics (MD) simulations also suggested a binding motif, LRTLA, for *Oryza* Tom20.³¹ Thus, it is reasonable to assume that the plant Tom20 adopts a similar dynamic, multiple-mode mechanism for the recognition of plant mitochondrial presequences by convergent evolution.

The tethering of target molecules on proteins is effective for the stabilization of transient complexes to obtain crystallographic snapshots of bound states with large residual motions. In the case of Tom20, the disulfide tether with a linker of an optimal length had no severely restrictive effects on the motions of the presequence peptide *in solution*, since a reasonable consensus sequence was obtained in the library experiments,²² and the existence of residual motions on a submillisecond time scale within the Tom20–presequence interface was revealed by NMR ¹⁵N relaxation analyses.²⁷ In contrast, *in crystal*, the amino acid residues in the linker region were involved in the crystal lattice formation, which effectively arrested the motions of the peptide into a particular pose. However, in general, an intermolecular covalent bond for tethering might excessively restrict the dynamics with a careless design or even facilitate artifactual poses in the worst cases.

An alternative method to obtain crystallographic snapshots of transient complexes involves the introduction of an intramolecular disulfide bond in peptidic ligands. The design of a peptide targeted to the human estrogen receptor is an instructive example.³² Estrogen receptor is a transcription factor that is activated by the binding of a steroid hormone, estrogen. The hormone-bound estrogen receptor binds to the LXXLL motif (L is leucine and X is any amino acid) in its cognate coactivator proteins. Interestingly, this motif is a subset of the Tom20-binding motif, $\phi\chi\chi\phi\phi$. The LXXLL sequence adopts an α -helical conformation, and the side chains of the three leucine residues are recognized simultaneously and strictly by three hydrophobic sites in the estrogen receptor, by a conventional key-and-lock mechanism.³³ Leduc et al. considered various designs of a disulfide bridge compatible with an α -helical conformation and found a short peptide containing D-Cys and L-Cys at the *i* and *i* + 3 positions embedded in the $X_iXLX_{i+3}XLL$ sequence was the best.³² This peptide analogue interacted with the human estrogen receptor more tightly than its linear counterpart. For convenience, we refer to this method as the “molecular stiffening” of a ligand peptide in this article. The crystal structure of the LBD domain of estrogen receptor α associated with estradiol and the stiffened peptide revealed that the peptide was bound to the binding groove on the LBD domain and adopted the expected amphiphilic helical conformation.³²

In this work, to assess the possibility of tethering artifacts, we determined the crystal structure of a Tom20–presequence complex after the cleavage of the intermolecular disulfide bond in crystals. We also determined the crystal structure of the tethered complex with a nonoptimized, longer linker. As an alternative method without tethering, we synthesized stiffened

peptides with an intramolecular disulfide bond and determined two crystal structures of the complex with the cytosolic domain of Tom20. These four crystal structures confirmed the validity of the previously determined tethered structures as unbiased poses and revealed a new pose, which provides a better understanding of the Tom20–presequence interactions. Thus, we have demonstrated the effectiveness of the molecular tethering and molecular stiffening techniques to capture snapshots of the dynamic equilibrium among the multiple bound states of transient protein–peptide interactions.

MATERIALS AND METHODS

Protein and Peptide Preparations. The core structure of the cytosolic domain of rat Tom20 (accession number Q62760), encompassing Asp59–Leu126, was produced as a GST-fusion protein in *E. coli* BL21(DE3) and was purified after PreScission protease cleavage as described.²⁶ The Cys100 residue was substituted with Ser to generate the Tom20C100S mutant. The ¹⁵N-labeled protein was produced by culturing *E. coli* cells in M9 minimum medium containing ¹⁵NH₄Cl. The peptide sequence (Gly¹²–Pro¹³–Arg¹⁴–Leu¹⁵–Ser¹⁶–Arg¹⁷–Leu¹⁸–Leu¹⁹–Ser²⁰), derived from the presequence (pALDH) of rat mitochondrial aldehyde dehydrogenase (accession number P11884), was used as the template for the peptides in this study (Tables 1 and 2). The residue numbering starts at 12, since the sequence corresponds to the C-terminal half of pALDH. Peptides were custom synthesized with an N-terminal acetyl group and a C-terminal amide group by Hayashi-Kasei (Osaka, Japan). The disulfide-bond-tethered complex of Tom20 with presequence peptides was prepared as described.²⁶ The intramolecular disulfide bond within the presequence peptides was formed by air oxidation, as follows. The peptides were dissolved in a 10 mM NH₄HCO₃ solution to a final concentration of 0.01 mg/L and were incubated at 277 K for 48 h. After lyophilization, the peptides were purified by reverse-phase HPLC chromatography. The disulfide bond formation was confirmed by MALDI-TOF mass spectrometry.

Crystallization. All crystallization was performed by the hanging drop vapor diffusion method, from equal volumes (1 μ L) of the protein and reservoir solutions. Crystals of the disulfide-bond-tethered complex of Tom20 and pALDH(S) were obtained at 303 K from the protein solution (15 mg/mL Tom20-SS-pALDH(S) in 10 mM HEPES-NaOH, pH 7.5) and the reservoir solution (0.09 M MES pH 6.0, 0.045 M MgCl₂, 24% PEG3350, and 10% ethylene glycol) in 5 days. The crystals were soaked in the reservoir solution containing 10 mM dithiothreitol (DTT) for 30 s just prior to the diffraction measurement. Crystals of the disulfide-bond-tethered complex of Tom20 and pALDH(Y5) were obtained at 293 K from the protein solution (15 mg/mL Tom20-SS-pALDH(Y5) in 10 mM MES-NaOH, pH 6.5) and the reservoir solution (0.1 M sodium acetate, pH 4.6, and 1 M ammonium dihydrogen phosphate) in 1 day. Cocrystals (form 1) of Tom20 and the disulfide-stiffened pALDH(cxxC) were obtained at 293 K from the protein solution (16 mg/mL Tom20 and a 20% molar excess of pALDH(cxxC) in 10 mM MES-NaOH, pH 6.5) and the reservoir solution (0.1 M HEPES-NaOH, pH 7.0, 10% isopropanol, and 20% PEG4000) in 3 days. Cocrystals (form 2) of the Tom20C100S and the disulfide-stiffened pALDH(cxxC) were obtained at 293 K from the protein solution (13 mg/mL Tom20C100S and a 20% molar excess of pALDH(cxxC) in 10 mM MES-NaOH, pH 6.5) and the

Table 1. Data Collection and Refinement Statistics

Tom20—preseq complex ^a	Tom20-S/pALDH(S)	Tom20-SS-pALDH(Y5)	Tom20/pALDH(cxxC) form 1	Tom20/pALDH(cxxC) form 2
Tom20 ^b	WT	WT	WT	C100S
pALDH ^c	pALDH(S) GPRL <u>S</u> RLLSAGC	pALDH(Y5) GPRL <u>S</u> RLLSYAGSGC	pALDH(cxxC) G-cyclo(cRLC)- <u>RLLS</u> YA	pALDH(cxxC) G-cyclo(cRLC)- <u>RLLS</u> YA
<i>data collection statistics</i>				
space group	P2 ₁	P3 ₁	I222	R32
cell parameters (Å)	<i>a</i> = 33.8, <i>b</i> = 27.7, <i>c</i> = 70.8, <i>β</i> = 102.7	<i>a</i> = <i>b</i> = 61.5, <i>c</i> = 98.34 (90, 90, 120)	<i>a</i> = 41.8, <i>b</i> = 77.4, <i>c</i> = 116.2 (90, 90, 120)	<i>a</i> = <i>b</i> = 99.60, <i>c</i> = 195.18, (90, 90, 120)
no. of molecules in AU	2	4	2	4
resolution range (Å)	50.0–2.00 (2.07–2.00)	30.0–1.90 (1.93–1.90)	30.0–2.20 (2.24–2.20)	50.0–2.10 (2.18–2.10)
unique reflections	8725	32732	9917	22101
redundancy	3.4 (2.4)	5.8 (5.7)	7.1 (7.2)	9.7 (9.2)
completeness (%)	98.3 (89.1)	99.9 (100)	99.9 (100)	99.7 (100)
<i>R</i> _{merge} (<i>I</i>) ^d	0.089 (0.296)	0.081 (0.587)	0.101 (0.561)	0.067 (0.496)
<i>I</i> /σ(<i>I</i>)	11.1 (2.4)	20.3 (2.5)	15.9 (3.5)	31.2 (5.6)
<i>refinement statistics</i>				
resolution range (Å)	50.0–2.00 (2.07–2.00)	27.0–1.90 (1.93–1.90)	28.4–2.20 (2.24–2.20)	28.9–2.10 (2.18–2.10)
<i>R</i> / <i>R</i> _{free}	0.2061/0.2507	0.1876/0.2185	0.2221/0.2755	0.2430/0.2870
rmsd ^e from ideality	0.011	0.028	0.022	0.024
bond length (Å)				
angles (deg)	1.421	2.193	1.902	2.006
PDB entry	3AWR	3AX2	3AX5	3AX3

^a “-” denotes a covalent bond, and “/” implies noncovalent interactions. ^b WT = the core structure of the cytosolic domain of rat Tom20, encompassing Asp59-Leu126. C100S = the mutant of Cys100 to serine. ^c pALDH = the C-terminal half of the presequence from rat mitochondrial aldehyde dehydrogenase. The Tom20 binding consensus is underlined. The D-cysteine residue is denoted by the symbol “c”. The spacer sequences are in italics. The N-terminal amino group is acetylated, and the C-terminal carboxyl group is amidated. ^d $R_{\text{merge}}(I) = (\sum |I_i - \langle I \rangle|) / \sum I_i$, where I_i is the intensity of the *i*th observation and $\langle I \rangle$ is the mean intensity. Values in parentheses refer to the outer shell. ^e rmsd = root-mean-square deviation.

reservoir solution (0.1 M Tris-HCl, pH 8.0, 0.2 M MgCl₂, and 30% PEG4000) in 1 day.

Data Collection and Structure Determination. The diffraction data were collected on beamline BL38B1 at the SPring-8, Harima, Japan, and on beamlines on PF-BLSA, PF-BL17A, and AR-NW12A at the Photon Factory, Tsukuba, Japan. The crystals were cooled at 95–100 K, using 10–20% ethylene glycol plus the mother liquor as a cryoprotectant. For the Tom20/pALDH(cxxC) form 2 crystal, Crystal Catcher (SOSHO Inc., Osaka, Japan) was used to mount the crystal without a cryoprotectant. The diffraction data were processed with the program HKL2000 ver. 0.98.698s.³⁴ Initial phases were generated by the molecular replacement method with the program Phaser MR in the CCP4 program package,³⁵ using the coordinates of the previously determined Tom20-SS-pALDH(A) (PDB: 2V1T) and Tom20-SS-pALDH(Y) (PDB: 2V1S) structures without the pALDH peptides as a search model. The crystal structures were refined with the program Refmac5 in the CCP4 package. Statistics for data collection and refinement are summarized in Table 1. The detailed version of Table 1 is in the Supporting Information (Table S1). The figures were prepared with PyMOL, version 1.3 (DeLano Scientific). The coordinates and structure factors have been deposited in the Protein Data Bank (PDB: 3AWR, 3AX2, 3AX3, 3AX5).

NMR Spectroscopy. NMR spectra were recorded at 298 K on a Bruker Avance 600 spectrometer equipped with a TXI cryoprobe. The NMR sample comprised 0.1 mM ¹⁵N-labeled Tom20C100S in 90% ¹H₂O/10% ²H₂O, containing 20 mM MOPS-NaOH, pH 7.0, and 50 mM NaCl. The presequence

Table 2. Dissociation Constants for the Core Domain of Tom20 with pALDH Peptide Analogues Determined by the NMR Titration Experiments

peptide name	presequence peptide ^a	<i>K</i> _d (μM) ^b
pALDH	GPRL <u>S</u> RLLSYA	250 ± 50 ^c
linear pALDH(cxxC) ^d	GcRLCRLLSYA	160 ± 20
pALDH(cxxC)	G-cyclo(cRLC)- <u>RLLS</u> YA	1.4 ± 0.5
pALDH(cxxh)	G-cyclo(cRLh)- <u>RLLS</u> YA	29 ± 6
pALDH(cxxC)L15S	G-cyclo(cRSC)- <u>RLLS</u> YA	270 ± 50 ^c
pALDH(cxxC)L18S	G-cyclo(cRLC)- <u>RLSS</u> YA	56 ± 5
pALDH(cxxC)L19S	G-cyclo(cRLC)- <u>RLSS</u> YA	140 ± 20

^a The template sequence was derived from the presequence of rat mitochondrial aldehyde dehydrogenase. The Tom20-binding consensus is underlined. The D-type cysteine and L-homocysteine residues are denoted by the symbols “c” and “h”, respectively. The N-terminal amino group is acetylated, and the C-terminal carboxyl group is amidated. ^b Calculated from the analysis of the ¹H–¹⁵N cross-peak of Thr113 of ¹⁵N-labeled Tom20. ^c The *K*_d value of the pALDH for the core domain (residues 59–126) of Tom20 is an order of magnitude larger than that for the cytosolic domain (residues 51–145) of Tom20 reported previously.²⁵ This is probably due to the removal of the fifth α-helix in the cytosolic domain for crystallization. ^d Without an intramolecular disulfide bridge. ^e From the ¹H–¹⁵N cross-peak of Val109.

peptides were added to the protein solution to monitor the binding at molar ratios of 0, 0.25, 0.5, 0.75, 1.0, 1.25, 1.5, 2.0, 2.5, and 3.0. The titration curves were analyzed with the program

xcrvfit ver. 4.0.12 (available at <http://www.bionmr.ualberta.ca/bds/software/xcrvfit/>).

Circular Dichroism Spectroscopy. CD spectra were recorded at ambient temperature with a J-820 spectropolarimeter (Jasco, Tokyo, Japan), using a 1 mm path length cell. Four scans ranging from 200 to 250 nm were measured with 0.17 mg/mL pALDH(cxxC) in 30 mM MES-NaOH, pH 6.0. The secondary structure content was estimated with the program JWSSE-480, from Jasco.

RESULTS AND DISCUSSION

Molecular Tethering Does Not Introduce Biases in the Presequence Poses. Mixing the core domain of the Tom20 protein with the presequence peptides did not generate any crystals, probably due to the large residual motions of the presequence peptides in the bound state, in addition to the weak affinity. The tethering of the presequence peptides to Tom20 by an intermolecular disulfide bond with a carefully designed linker was required to obtain diffraction quality cocrystals. Once the cocrystals form, the disulfide tether may be unnecessary for maintaining the crystal contacts. As an ideal outcome, after the reduction of the disulfide bond, the crystal still diffracted but revealed poor density for the bound presequence peptide, reflecting the residual mobility in the binding pocket of Tom20. Actually, the *in situ* reductive cleavage of the disulfide bond in the Tom20-SS-pALDH(S) crystals (i.e., a disulfide bond tethered complex with a linker containing Ser at the X position, which has a virtually identical structure to Tom20-SS-pALDH-(A), Table 1) did not cause any structural changes even around the disulfide bond, except that the C-terminal cysteine residue of the peptide became disordered and invisible (Figure 1B). This suggests that the driving force that fixes the presequence in one pose in the crystal is not the disulfide bond, but based on noncovalent interactions between Tom20 and the presequence, including the spacer region. Note that attempts to cleave the disulfide bond in another pose within the Tom20-SS-pALDH-(Y) crystals (with a linker containing Tyr at the X position) were unsuccessful. Unfortunately, these results do not provide definitive ideas about the dynamic aspects of the binding mode of the presequence peptide but offer a valuable hint for future conceivable crystallographic experiments using disulfide bond tethered Tom20–presequence complexes.

In another experiment, a five-residue spacer (XAGSG), instead of the optimized three-residue spacer (XAG), was used to prepare the tethered complex. The insertion of the two extra residues in the spacer considerably weakened the affinity to Tom20.²² We obtained crystals of tethered complexes with two different linkers, Ala or Tyr at the X-position of the five-residue spacer, but only pALDH(Y5) (five-residue spacer containing Tyr) produced diffraction quality crystals. The crystal belonged to a different space group from the crystal of Tom20-SS-pALDH(Y) containing the optimized three-residue spacer (Table 1 and Table S1). The poses are not completely identical to each other, and the directions of the helical axis are slightly different, but the recognition modes of the three leucine residues are the same in the two poses (Figure 1C). The two extra residues in the spacer region form an extended part of the α -helical structure of the presequence. This result demonstrates that the length of the linker is not critical for the selection of a particular pose upon crystallization.

An $i, i + 3$ Disulfide Bridge within the Presequence Enhances the Affinity to Tom20. The proper incorporation of an intramolecular disulfide bond within a presequence peptide is expected to increase the affinity to Tom20 by the loss of entropy in the free states of the peptide. Ideally, the disulfide bond does not influence the bound states and only restricts the freedom of the peptide in the free states. In the case of Tom20, the disulfide bridge should be compatible with an α -helical conformation. According to the previous successful design for the estrogen receptor,³² a pair of cysteine residues was incorporated at the i and $i + 3$ positions of Gly-Cys(i)-Arg-Leu-Cys($i+3$)-Arg-Leu-Leu-Ser-Tyr-Ala. The first cysteine was a D-type, and second one was the usual L-type. The three hydrophobic leucine residues comprising the consensus motif were maintained. The peptide is referred to as pALDH(cxxC), where c and C denote the D-cysteine and L-cysteine residues, respectively. The CD measurements revealed that the disulfide bridge slightly increased the helical content of pALDH(cxxC) from 0 to 5%, indicating that the pALDH(cxxC) peptide showed little helical character in the absence of Tom20 (Figure S1 of Supporting Information). The L-cysteine can be replaced by L-homocysteine, which has an extra methylene group in the side chain, for the expansion of the disulfide bridge loop size, and the peptide is referred to as pALDH(cxxh). We evaluated the binding affinity of these presequence analogues to Tom20 by NMR titration experiments (Figure 2A). We prepared ¹⁵N-labeled Tom20 and recorded [¹H, ¹⁵N]HSQC spectra as a function of the molar ratio of the added presequence peptides (Figure S2 of Supporting Information). The cross-peaks moved in the fast exchange regime on the NMR chemical shift time scale during the titration. The D-Cys, L-Cys, $i, i + 3$ motif increased the affinity by more than 100-fold as compared to the same peptide without a disulfide bridge and to the original pALDH sequence (Table 2). The L-homocysteine residue at the $i + 3$ position also enhanced the affinity, but the enhancement was not as high as the L-cysteine at the $i + 3$ position.

Disulfide-Bridged Peptides Correctly Interact with Tom20 in Solution. We checked whether the disulfide bridging skewed the binding mode of the presequences. The chemical shift changes of each amide group of ¹⁵N-labeled Tom20, induced by the addition of an equimolar amount of pALDH(cxxC), were mapped onto the three-dimensional structure of Tom20 (Figure 2B). The residues with large chemical shift changes were located on the molecular surface where the original pALDH peptide bound in solution.²⁵ We then examined the effects of replacing each of the three leucine residues with serine in the Tom20-binding consensus of the pALDH(cxxC) peptide. The NMR titration experiments were repeated, and the K_d values were calculated (Table 2). All of the amino acid replacements with Ser resulted in affinity reductions ranging from 40- to 200-fold, indicating that the binding of the pALDH(cxxC) peptide to Tom20 is dependent on the three hydrophobic residues in the Tom20-binding consensus. In summary, the incorporation of a disulfide bridge between the i and $i + 3$ positions in the Tom20-binding consensus enhanced the affinity to Tom20, without changing the binding mode in solution.

The Same Pose of the Presequence Was Obtained by the Molecular Stiffening Method. Crystallization screenings of the disulfide-bridged presequence peptides, pALDH(cxxC) and its Ser mutants, and pALDH(cxxh), were performed in the presence of the cytosolic domain of Tom20. Only the pALDH(cxxC) peptide generated crystals under several crystallization conditions.

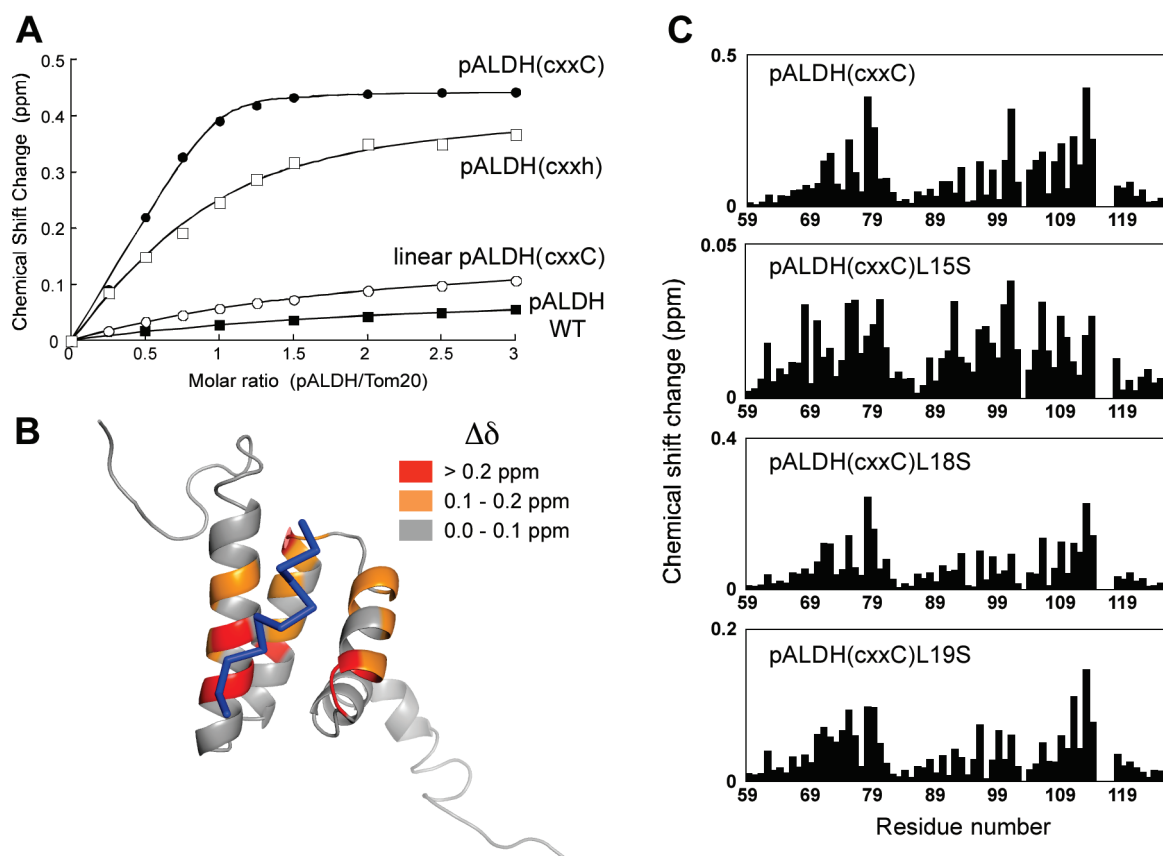


Figure 2. NMR experiments to verify the interactions of the disulfide-stiffened peptides with Tom20 in solution. (A) NMR titration curves to determine the affinities of the presequence peptides for Tom20: pALDH(cxxC) (black circles), pALDH(cxxh) (white squares), linear pALDH(cxxC) (white circles), pALDH WT (black squares). Best fit curves, calculated with the program xcrvfit, are shown. The calculated K_d values are listed in Table 2. (B) Mapping of the chemical shift perturbations of the ^{15}N -Tom20 backbone amides upon binding to the pALDH(cxxC) peptide, on the NMR structure of Tom20/pALDH (PDB: 1OM2). A combined index of the chemical shift change of each amide cross-peak was calculated according to the equation $\Delta\delta = [\Delta\delta(^1\text{H})^2 + (\Delta\delta(^{15}\text{N})/5)^2]^{1/2}$ at the molar ratio of 1:1. (C) Chemical shift changes of the backbone amides of the ^{15}N -labeled Tom20 by the addition of the pALDH(cxxC) peptides with substitution of Leu by Ser at the molar ratio of 1:1 as a function of the residue number of the Tom20 protein.

Crystals in the space groups *I*222 and *R*32 were obtained, and their structures were determined (Table 1). One structure (*I*222) was determined at a resolution of 2.2 Å. There were two Tom20/pALDH(cxxC) complexes in the asymmetric unit of the crystal. Note that “/” means noncovalent interactions between Tom20 and the presequence. The pose in the structure of the complex was almost indistinguishable from the previous pose of the pALDH(Y) peptide, determined by the molecular tethering method (Figure 3A). The pALDH(cxxC) peptide adopted an α -helical conformation in the segment Cys16-Leu19 but exhibited a tighter twist in the helical conformation in the segment D-Cys13-Leu15, induced by the disulfide bond between D-Cys13 and Cys16. This distortion is necessary for the higher affinity because the longer disulfide bridge formed by the D-Cys and L-homocysteine pair exhibited weaker affinity (Table 2). The fact that we obtained the same pose of the presequence, irrespective of the method for complex state stabilization, indicates that the poses of the presequence are principally selected by the noncovalent interactions between Tom20 and the presequence.

It should be noted that the other complex in the same crystal had a completely different pose (Figure 3B). In addition to its extremely high *B* factors ($>50 \text{ Å}^2$), the inconsistency of the pose with the solution NMR data demonstrates that this pose is of little significance in the Tom20–presequence interactions. Two

types of solution NMR data are available: chemical shift perturbation study in Figure 2 and spin-labeling experiment in the previous study.²³ The latter provided the geometric information on the orientation of the presequence peptides in the binding groove of Tom20. Obviously, the N–C orientation determined by the spin-labeling analysis is opposite to that of the second pose in the Tom20/pALDH(cxxC) crystal. This “irregular” pose reminds us of the importance of careful interpretation of the crystal structures as a snapshot.

A New Pose of the Presequence Was Revealed by the Molecular Stiffening Method. The structure of the other crystals (space group *R*32) obtained under different crystallization conditions was determined at a resolution of 2.1 Å (Tom20/pALDH(cxxC) form 2 in Table 1). The asymmetric unit contains four Tom20/pALDH(cxxC) complexes. The four structures are almost identical to each other, with an average root-mean-square distance of 0.63 Å over 77 C α atoms of Tom20 and the peptide. Apparently, the new pose resembles the previous pose seen in the tethered Tom20-SS-pALDH(A) structure, but the movement of the presequence along the helical axis results in a completely different interaction mode with Tom20 (Figure 4A). The new pose is also different from the previous pose in the tethered Tom20-SS-pALDH(Y) structure and thus exhibits a unique interaction mode (Figure 4B).

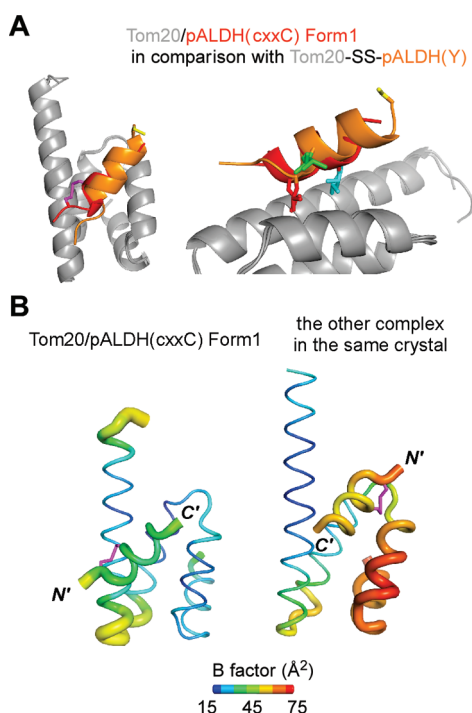


Figure 3. Crystal structure of Tom20/pALDH(cxxC) form 1. (A) Superposition of the structures of Tom20/pALDH(cxxC) form 1 and Tom20-SS-pALDH(Y). The 69 C α atoms of Tom20 were superposed with an rms distance of 0.43 Å. Independently of the stabilization method, the pose and the interaction mode of the presequence peptide are almost indistinguishable for the two structures. (B) B factor putty tube representation of the two complex structures in the Tom20/pALDH(cxxC) form 1 crystal. The 69 C α atoms of Tom20 were superposed with an rms distance of 1.1 Å. The second nonproductive complex (right) has high B factors (>50 Å²) as compared with the structure of Tom20/pALDH(cxxC) form 1 (left). The N–C orientation of the α -helix is opposite between the first pose and the second “irregular” pose. The N- and C-termini of the presequence peptide are designated with apostrophes.

Revised Version of the Dynamic, Multiple Modes of Tom20–Presequence Interactions. Figure 5 shows a schematic view of the dynamic, multiple modes of presequence recognition by Tom20. In addition to the two previous poses revealed by the molecular tethering method, the new pose (Tom20/pALDH(cxxC) form 2, Figure 4) added a third pose in the revised scheme. It is tempting to speculate that the new pose might be an intermediate state between the two poses. The uniqueness of the multiple modes of recognition by Tom20 is that each pose recognizes different partial features of the Tom20-binding consensus, $\phi_1\chi\chi\phi_4\phi_5$: the two hydrophobic side chains with different combinations, (ϕ_1,ϕ_4) , (ϕ_1,ϕ_5) , and (ϕ_4,ϕ_5) , of the three Leu residues are recognized by the two hydrophobic sites on Tom20 in each pose. We assume that a dynamic equilibrium exists between the three poses, for the full recognition of the three hydrophobic residues. One would expect that the limitation of the recognition motif to include only two of the three hydrophobic residues would bias the dynamic equilibrium toward a particular pose. Figure 2C shows the chemical shift changes of the backbone amides of Tom20 by the addition of pALDH(cxxC) peptides with substitution of one of the three Leu by Ser. The overall pattern of the chemical shift perturbation is different for each peptide variant, suggesting biased distribution

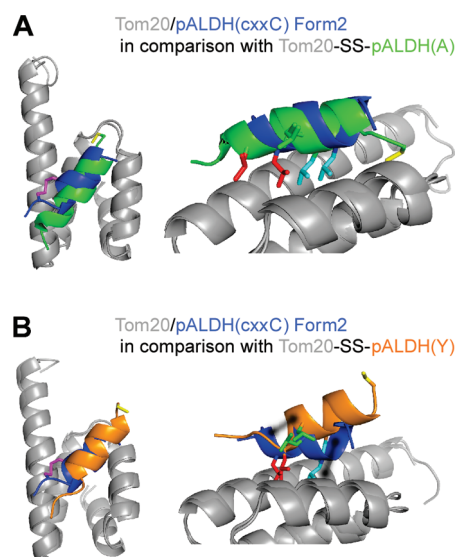


Figure 4. Crystal structure of Tom20/pALDH(cxxC) form 2, with a new pose. (A) Superposition of the structures of Tom20/pALDH(cxxC) form 2 and Tom20-SS-pALDH(A). The 68 C α atoms of Tom20 were superposed with an rms distance of 0.76 Å. (B) Superposition of the structures of Tom20/pALDH(cxxC) form 2 and Tom20-SS-pALDH(Y). The 68 C α atoms of Tom20 were superposed with an rms distance of 0.79 Å.

of residual motions to the corresponding pose. Naturally, the number of poses is not limited to three, and other poses will be found by different tethering and stiffening designs and under different crystallization conditions in the future. We propose that the dynamic, multiple-mode interaction is the molecular mechanism facilitating the promiscuous binding of the Tom20 receptor to diverse mitochondrial presequences with similar affinities.

Generality of Dynamic, Multiple Mode Interactions. In the present study, we described our efforts to assess the validity of the molecular tethering and stiffening techniques to obtain structural information at an atomic resolution from transient protein–protein interactions. There are numerous promiscuous protein–protein interactions, in which the flexibility, dynamics, mobility, configurational/conformational entropy, plasticity, and malleability in the bound/complex states are suggested to be important for binding, recognition, or catalysis for a variety of different ligands/substrates using a single binding/active site.^{6,7} One good example is the regulatory subunit of protein kinase A (PKA-R), which interacts with A-kinase anchoring proteins (AKAPs).³⁶ The multiple mode recognition was suggested as a molecular mechanism for the promiscuity, and the dynamic aspect is necessary to maintain the high affinity. PKA-R binds to a segment of the AKAP protein in an amphiphilic, α -helical conformation. MD simulations revealed that the large hydrophobic binding surface of the D/D domain of the PKA-R allows multiple poses of the AKAP peptide in the binding groove in order to sample multiple contact modes. This dynamic feature increases the configurational entropy upon binding and thus ensures high affinity. Concurrently, the selection of a suitable interaction mode unique to each partner peptide, from multiple modes, provides the structural basis for the promiscuous association with a wide variety of target partners. The key feature for the promiscuity was ascribed to the involvement of flexible aliphatic

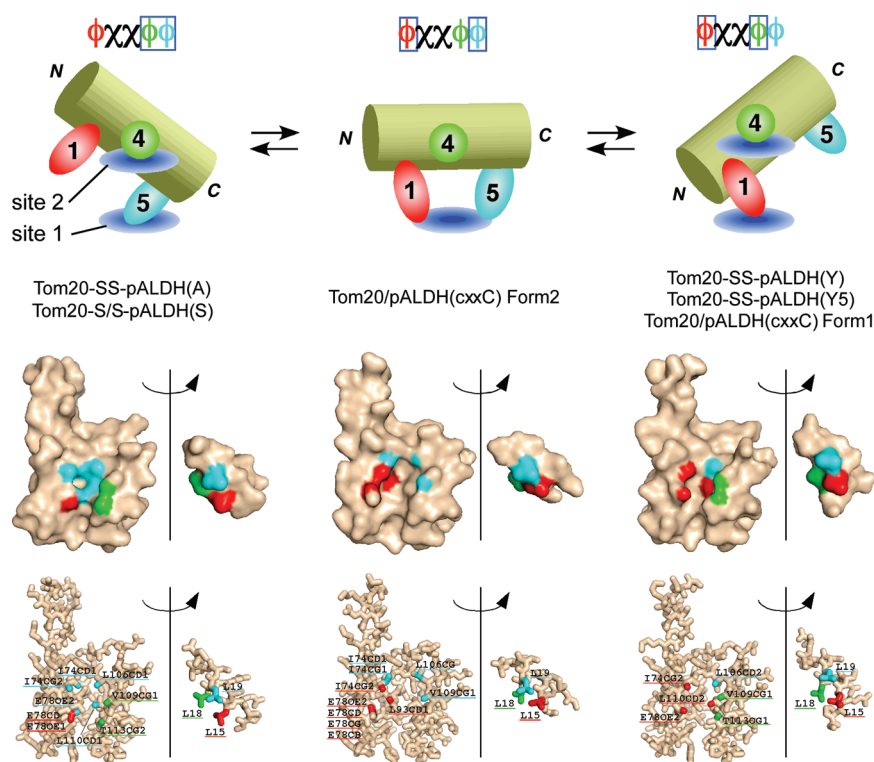


Figure 5. Schematic representation of the dynamic recognition of the three hydrophobic side chains in the mitochondrial presequence by Tom20. The presequence peptide adopts an α -helical conformation in the bound states. The helices are drawn as cylinders, to imply the firmness of the helical structure. The three hydrophobic side chains in the 5-residue Tom20-binding consensus motif, at positions 1, 4, and 5, are colored red, green, and cyan, respectively. They are recognized by one of the two hydrophobic pockets (blue disks): site 1 consisting of the side chains of Ile74, Leu106, and Leu110 and site 2 consisting of the side chains of Val19 and Thr113. The three poses are assumed to be in a rapid equilibrium, and the side chain at position 4 functions as a fulcrum. It is likely that other bound poses exist, and they are in equilibrium with the three poses. Open-book representations show the contact residues at the Tom20–presequence interface. Two atoms are defined as being in contact if the distance between them is less than 4.0 Å. The surface and atoms of Tom20 that contacts one of the side chain atoms of the three leucine residues of the presequence have the same color.

side chains (Leu, Val, Thr), and the absence of rigid aromatic rings (Trp, Phe, Tyr), at the molecular interface. The same bias exists in the hydrophobic amino acid composition at the binding surface of Tom20.²⁵ In summary, the interaction between PKA-R and AKAP shares many common aspects with that between Tom20 and presequences.

It should be noted here that the two methods presented here are useful to collect snapshots of transient protein–protein interactions but do not guarantee the capture of major substates, i.e., no warranty for a proper sampling of the interaction space. The pose on the right in Figure 5 is probably a major substate because two independent methods resulted in the same pose. In contrast, the pose at the center in Figure 5 probably represents a minor substate because one hydrophobic site of Tom20 is empty, and thus the pose seems less stable. A new experimental approach that allows a presequence peptide in the binding pocket to be free from crystal packing effects is necessary to solve the sampling problem.

Among the many similar promiscuous protein–protein interactions, the interactions of Tom20 are unique because the poses of the presequence peptide in complexes with Tom20 exhibited partial recognition of the Tom20-binding consensus motif. Although few reports have mentioned such partial recognition, this feature may be a key to understand the promiscuity of protein–protein interactions. In this context, for collecting meaningful poses, the careful design of tethering and stiffening is critical to preserve the large

intrinsic movements of the ligand in the bound states. Library approaches are useful to find a good design.^{18,22,37}

■ ASSOCIATED CONTENT

S Supporting Information. Table of the detailed version of Table 1 (data collection and refinement statistics) and two figures of the CD spectra of pALDH(cxxC) in solution and the NMR titration experiment showing the changes in the [¹H, ¹⁵N]HSQC spectrum of Tom20 upon the gradual addition of pALDH(cxxC). This material is available free of charge via the Internet at <http://pubs.acs.org>.

■ AUTHOR INFORMATION

Corresponding Author

*Phone: + 81-92-642-6968. Fax: + 81-92-642-6764. E-mail: kohda@bioreg.kyushu-u.ac.jp.

Present Addresses

^{||}Laboratory of Biomolecular Science, Faculty of Pharmaceutical Sciences, Hokkaido University, Nishi 6, Kita 12, Kita-ku, Sapporo 060-0812, Japan.

Funding Sources

This study was supported by Grants-in-Aid for Scientific Research on Innovative Areas (21121003), and the Targeted Proteins Research Program (TPRP) from the Ministry of

Education, Culture, Sports, Science and Technology (MEXT) of Japan (D.K.).

ACKNOWLEDGMENT

We thank Dr. Tatsuya Nishino and Professor Kosuke Morikawa (Osaka University) for their generous assistance with the initial setup of the crystallographic analysis and Professor Toshiya Endo (Nagoya University) for helpful discussions. We thank the staffs at beamline BL38B1 of the SPring-8 and at beamlines PF-BL5A, PF-BL17A, and AR-NW12A of the Photon Factory. The experiments at the SPring-8 were approved by the Japan Synchrotron Radiation Research Institute (JASRI), as proposal 2007A1469. The experiments at the Photon Factory were approved by the High Energy Accelerator Research Organization (KEK), as proposals 2007G208 and 2009G021.

ABBREVIATIONS

AKAP, A-kinase anchoring protein; ALDH, aldehyde dehydrogenase; CD, circular dichroism; DTT, dithiothreitol; MD, molecular dynamics; pALDH, presequence of ALDH; PKA-R, the regulatory subunit of protein kinase A; TOM, translocase of outer mitochondrial membrane; TPR, tetratricopeptide repeat; WT, wild-type.

REFERENCES

- (1) Bruce, B. D. (2001) The paradox of plastid transit peptides: conservation of function despite divergence in primary structure. *Biochim. Biophys. Acta* 1541, 2–21.
- (2) Pandey, K. N. (2010) Small peptide recognition sequence for intracellular sorting. *Curr. Opin. Biotechnol.* 21, 611–620.
- (3) Christophe, D., Christophe-Hobertus, C., and Pichon, B. (2000) Nuclear targeting of proteins: how many different signals? *Cell Signal* 12, 337–341.
- (4) Schatz, G., and Dobberstein, B. (1996) Common principles of protein translocation across membranes. *Science* 271, 1519–1526.
- (5) Pfanner, N. (2000) Protein sorting: recognizing mitochondrial presequences. *Curr. Biol.* 10, R412–415.
- (6) Erijman, A., Aizner, Y., and Shifman, J. M. (2011) Multispecific recognition: mechanism, evolution, and design. *Biochemistry* 50, 602–611.
- (7) Schreiber, G., and Keating, A. E. (2011) Protein binding specificity versus promiscuity. *Curr. Opin. Struct. Biol.* 21, 50–61.
- (8) Vaynberg, J., Fukuda, T., Chen, K., Vinogradova, O., Velyvis, A., Tu, Y., Ng, L., Wu, C., and Qin, J. (2005) Structure of an ultraweak protein-protein complex and its crucial role in regulation of cell morphology and motility. *Mol. Cell* 17, 513–523.
- (9) Meenan, N. A., Sharma, A., Fleishman, S. J., Macdonald, C. J., Morel, B., Boetzel, R., Moore, G. R., Baker, D., and Kleinhous, C. (2010) The structural and energetic basis for high selectivity in a high-affinity protein-protein interaction. *Proc. Natl. Acad. Sci. U.S.A.* 107, 10080–10085.
- (10) Huang, H., Harrison, S. C., and Verdine, G. L. (2000) Trapping of a catalytic HIV reverse transcriptase*template:primer complex through a disulfide bond. *Chem. Biol.* 7, 355–364.
- (11) Fremont, D. H., Hendrickson, W. A., Marrack, P., and Kappler, J. (1996) Structures of an MHC class II molecule with covalently bound single peptides. *Science* 272, 1001–1004.
- (12) Hennecke, J., Carfi, A., and Wiley, D. C. (2000) Structure of a covalently stabilized complex of a human alphabeta T-cell receptor, influenza HA peptide and MHC class II molecule, HLA-DR1. *EMBO J.* 19, 5611–5624.

- (13) Pellegrini, L., Yu, D. S., Lo, T., Anand, S., Lee, M., Blundell, T. L., and Venkitaraman, A. R. (2002) Insights into DNA recombination from the structure of a RAD51-BRCA2 complex. *Nature* 420, 287–293.
- (14) Freund, C., Kuhne, R., Park, S., Thiemke, K., Reinherz, E. L., and Wagner, G. (2003) Structural investigations of a GYF domain covalently linked to a proline-rich peptide. *J. Biomol. NMR* 27, 143–149.
- (15) Janda, C. Y., Li, J., Oubridge, C., Hernandez, H., Robinson, C. V., and Nagai, K. (2010) Recognition of a signal peptide by the signal recognition particle. *Nature* 465, 507–510.
- (16) Jiang, J., Maes, E. G., Taylor, A. B., Wang, L., Hinck, A. P., Lafer, E. M., and Sousa, R. (2007) Structural basis of J cochaperone binding and regulation of Hsp70. *Mol. Cell* 28, 422–433.
- (17) Guo, M., Bhaskar, B., Li, H., Barrows, T. P., and Poulos, T. L. (2004) Crystal structure and characterization of a cytochrome c peroxidase-cytochrome c site-specific cross-link. *Proc. Natl. Acad. Sci. U.S.A.* 101, 5940–5945.
- (18) Corn, J. E., and Berger, J. M. (2007) FASTDXL: a generalized screen to trap disulfide-stabilized complexes for use in structural studies. *Structure* 15, 773–780.
- (19) Chacinska, A., Koehler, C. M., Milenkovic, D., Lithgow, T., and Pfanner, N. (2009) Importing mitochondrial proteins: machineries and mechanisms. *Cell* 138, 628–644.
- (20) Dolezal, P., Likic, V., Tachezy, J., and Lithgow, T. (2006) Evolution of the molecular machines for protein import into mitochondria. *Science* 313, 314–318.
- (21) von Heijne, G. (1986) Mitochondrial targeting sequences may form amphiphilic helices. *EMBO J.* 5, 1335–1342.
- (22) Obita, T., Muto, T., Endo, T., and Kohda, D. (2003) Peptide library approach with a disulfide tether to refine the Tom20 recognition motif in mitochondrial presequences. *J. Mol. Biol.* 328, 495–504.
- (23) Muto, T., Obita, T., Abe, Y., Shodai, T., Endo, T., and Kohda, D. (2001) NMR identification of the Tom20 binding segment in mitochondrial presequences. *J. Mol. Biol.* 306, 137–143.
- (24) Yamamoto, H., Itoh, N., Kawano, S., Yatsukawa, Y., Momose, T., Makio, T., Matsunaga, M., Yokota, M., Esaki, M., Shodai, T., Kohda, D., Hobbs, A. E., Jensen, R. E., and Endo, T. (2011) Dual role of the receptor Tom20 in specificity and efficiency of protein import into mitochondria. *Proc. Natl. Acad. Sci. U.S.A.* 108, 91–96.
- (25) Abe, Y., Shodai, T., Muto, T., Mihara, K., Torii, H., Nishikawa, S., Endo, T., and Kohda, D. (2000) Structural basis of presequence recognition by the mitochondrial protein import receptor Tom20. *Cell* 100, 551–560.
- (26) Igura, M., Ose, T., Obita, T., Sato, C., Maenaka, K., Endo, and Kohda, D. (2005) Crystallization and preliminary X-ray analysis of mitochondrial presequence receptor Tom20 in complex with a presequence from aldehyde dehydrogenase. *Acta Crystallogr. F61*, 514–517.
- (27) Saitoh, T., Igura, M., Obita, T., Ose, T., Kojima, R., Maenaka, K., Endo, T., and Kohda, D. (2007) Tom20 recognizes mitochondrial presequences through dynamic equilibrium among multiple bound states. *EMBO J.* 26, 4777–4787.
- (28) Perry, A. J., Rimmer, K. A., Mertens, H. D., Waller, R. F., Mulhern, T. D., Lithgow, T., and Gooley, P. R. (2008) Structure, topology and function of the translocase of the outer membrane of mitochondria. *Plant Physiol. Biochem.* 46, 265–274.
- (29) Perry, A. J., Hulett, J. M., Likic, V. A., Lithgow, T., and Gooley, P. R. (2006) Convergent evolution of receptors for protein import into mitochondria. *Curr. Biol.* 16, 221–229.
- (30) Rimmer, K. A., Foo, J. H., Ng, A., Petrie, E. J., Shilling, P. J., Perry, A. J., Mertens, H. D., Lithgow, T., Mulhern, T. D., and Gooley, P. R. (2011) Recognition of mitochondrial targeting sequences by the import receptors Tom20 and Tom22. *J. Mol. Biol.* 405, 804–818.
- (31) Zhang, Y., Baaden, M., Yan, J., Shao, J., Qiu, S., Wu, Y., and Ding, Y. (2010) The molecular recognition mechanism for superoxide dismutase presequence binding to the mitochondrial protein import receptor Tom20 from *Oryza sativa* involves an LRTLA motif. *J. Phys. Chem. B* 114, 13839–13846.
- (32) Leduc, A. M., Trent, J. O., Wittliff, J. L., Bramlett, K. S., Briggs, S. L., Chirgadze, N. Y., Wang, Y., Burris, T. P., and Spatola, A. F. (2003)

Helix-stabilized cyclic peptides as selective inhibitors of steroid receptor-coactivator interactions. *Proc. Natl. Acad. Sci. U.S.A.* 100, 11273–11278.

(33) Shiau, A. K., Barstad, D., Loria, P. M., Cheng, L., Kushner, P. J., Agard, D. A., and Greene, G. L. (1998) The structural basis of estrogen receptor/coactivator recognition and the antagonism of this interaction by tamoxifen. *Cell* 95, 927–937.

(34) Otwinowski, Z., and Minor, W. (1997) Processing of X-ray diffraction data collected in oscillation mode. *Methods Enzymol.* 276, 307–326.

(35) Collaborative Computational Project 4 (1994) The CCP4 suite: programs for protein crystallography. *Acta Crystallogr., Sect. D: Biol. Crystallogr.* 50, 760–763.

(36) Chang, C. E., McLaughlin, W. A., Baron, R., Wang, W., and McCammon, J. A. (2008) Entropic contributions and the influence of the hydrophobic environment in promiscuous protein-protein association. *Proc. Natl. Acad. Sci. U.S.A.* 105, 7456–7461.

(37) Erlanson, D. A., Braisted, A. C., Raphael, D. R., Randal, M., Stroud, R. M., Gordon, E. M., and Wells, J. A. (2000) Site-directed ligand discovery. *Proc. Natl. Acad. Sci. U.S.A.* 97, 9367–9372.